Research Article

Jun Ma* and Zhifang Zhou

Origin of the low-medium temperature hot springs around Nanjing, China

https://doi.org/10.1515/geo-2020-0269
received September 28, 2020; accepted June 18, 2021

Abstract: The exploration of the origin of hot spring is the basis of its development and utilization. There are many low-medium temperature hot springs in Nanjing and its surrounding karst landform areas, such as the Tangshan, Tangquan, Lunshan, and Xiangquan hot springs. This article discusses the origin characters of the Lunshan hot spring with geological condition analysis, hydrogeochemical data, and isotope data. The results show that the hot water is SO_4–Ca type in Lunshan area, and the cation content of SO_4 is high, which are related to the deep hydrogeological conditions of the circulation in the limestone. Carbonate and anhydrite dissolutions occur in the groundwater circulation process, and they also dominate the water–rock interaction processes in the geothermal reservoir of Lunshan. The hot water rising channels are deeply affected by the NW and SN faults. Schematic diagrams of the conceptual model of the geothermal water circulation in Lunshan are plotted. The origin of Tangshan, Tangquan, and Xiangquan hot springs are similar to the Lunshan hot spring. In general, the geothermal water in karst landforms around Nanjing mainly runs through the carbonate rock area and is exposed near the core of the anticlinal structure of karst strata, forming SO_4–Ca/SO_4–Ca–Mg type hot spring with the water temperature less than 60°C. The characters of the hot springs around Nanjing are similar, which are helpful for the further research, development, and management of the geothermal water resources in this region.

Keywords: hot spring, karst, geothermal water resources, hydrochemistry, isotope, China

1 Introduction

In these days, all over the world, the coal is still one of the most effective non-renewable resources for the production of electricity [1]. The exploitation and utilization of renewable resources (such as geothermal resources) can greatly reduce the consumption of coal, and it is significant to reduce the pressure of energy shortage and protect the ecological environment. Hot spring is a special renewable energy, which is one of the earliest geothermal resources to be developed. In karst landform area, when thermal water moves through soluble rock and creates cave systems, hot springs easily occur with suitable geological conditions [2]. Springs are usually among the most characteristic features of karst areas [3]. Karst areas where springs with elevated temperatures occur can be termed as thermal karst, and deep carbonate rock aquifers are probably the most important thermal water resources outside of volcanic areas [4]. Faults can form conduits or barriers, but their hydraulic function depends on several factors and is often difficult to predict [5]. Faults, fractures, and temperature-induced density gradients are the major controls on groundwater flow, and water circulation is generally gravity-driven caused by topographic gradients in the thermal karst systems [4].

Geological and hydrogeological investigations play an important role in establishing the hydrogeological properties of the lithologic units and in identifying possible reservoirs and cap rocks [6]. The formation of hot springs needs four important elements: water resource, pathway and rising channels of the thermal groundwater, thermal reservoir, and cap rock. The porosities and permeabilities of the various rocks are different [7], which can be used to distinguish reservoir rock and cap rock. In addition, water–rock interaction phenomena are the origin of the spatial variation of groundwater geochemistry [8], which is usually studied with hydrogeochemical and isotopic methods. Systematic hydrogeochemical and isotopic methods are essential in the studies of geothermal systems [9–11], and different aspects of a geothermal/groundwater system can be unveiled with different hydrogeochemical

* **Corresponding author: Jun Ma,** School of Earth Sciences and Engineering, Hohai University, No. 8 Focheng West Road, Nanjing 211100, China, e-mail: majun0108@hhu.edu.cn
Zhifang Zhou: School of Earth Sciences and Engineering, Hohai University, No. 8 Focheng West Road, Nanjing 211100, China, e-mail: zhouzf@hhu.edu.cn

and isotopic methods [12]. The widely applicable fundamental tools for studying thermal water include regional scale hydraulics, water chemistry, ^{2}H and ^{18}O isotopic composition, and geothermometry [13]. Geochemical and isotope methods are also effective in further studying the water source and circulation of groundwater and the temperature of underground thermal reservoir in karst areas. For examples, major ion concentrations in 404 springs in carbonate strata in the Sierra Madre Oriental (Mexico), the Rocky Mountains Front Range (Canada), and the Peak District (England) were found to exhibit a wide range in sulfate values, and the results showed that there is a direct relationship between sulfate concentration and spring temperature, and an inverse relationship with discharge [14]. The geochemical cycle of CO_2 and the hydrological cycle in the Taroko Gorge karst area, Taiwan, are discussed using chemical composition data of the natural water, together with stable isotope ratios of carbon and oxygen of the water and soil CO_2 [15]. Tracing fluid connections and basement interactions via chemical and isotopic compositions (such as $^{87}Sr/^{86}Sr$) are used in research of low enthalpy Na-chloride waters from the Lunigiana and Garfagnana grabens, Northern Apennines, Italy [16]. A conceptual model of regional scale groundwater flow for the thermal water is proposed in the carbonate formation in Chongqing, China, and this study is focused on characterizing the geochemistry of thermal water in the carbonate rock aquifer in the main urban area of Chongqing [13]. The major element chemistry and the isotope composition (δD, $\delta^{18}O$, $^{87}Sr/^{86}Sr$, and $\delta^{11}B$) of groundwater are used to study the thermal springs near the low-enthalpy geothermal system near the city of Viterbo in the Cimino-Vico volcanic district of west-central Italy [17].

Karst landforms are widely distributed in the areas surrounding Nanjing city in China, where low-medium temperature karst hot springs are also regularly distributed on both sides of the Yangtze River, including the Tangshan hot springs in the Tangshan Mountain of Nanjing, Lunshan hot springs in the Lunshan Mountain of Zhenjiang, Tangquan hot springs in the Pukou District of Nanjing, and Xiangquan hot springs in He County. The development of geothermal water resources in the Tangshan area of Nanjing has a history of more than 1,500 years. Nine geothermal wells have a banded distribution along the northeast direction in the eastern part of the Tangshan Mountain, and among them, the most famous geothermal well is the Jiangjieshi Villa Hot Spring [18]. Since 1959, many exploration works have been carried out around the Tangshan area to meet the needs of development in different periods. Luan and Qiu [19] proposed that the hot springs in Tangshan area of Nanjing city belong to the low-medium temperature convective geothermal system, and they performed a qualitative analysis of their genesis through geological conditions and geothermal background. Zhao and Zhu [20] conducted a preliminary analysis of the regional geological conditions, drill holes, and distribution of geothermal wells in the Tangshan hot spring area. The origin model and resource prospects of geothermal water in this area were discussed. Li et al. [21] further analyzed the anticline structure and thermal reservoir distribution in this area according to the magnetotelluric sounding data in the Tangshan hot spring area, which provided a basis for solving the heat source problem. Zou et al. [22] described a origin model of geothermal water in the Tangshan hot spring area based on the previous studies and performed quantitative calculations and analyses using the silicon enthalpy diagram method. A cross-sectional sketch of a genesis model of hot springs with a water circulation depth at 2.6–2.9 km and the geothermal water flowing upward in Tangshan hot spring area through the Tangshan-Dongchangjie Fault in the intersection zones of the NW-and NE-striking faults was plotted. Lu et al. [12] used chemical and isotopic tracers ($\delta^{2}H$, $\delta^{18}O$, ^{34}S, $^{87}Sr/^{86}Sr$, $\delta^{13}C$, ^{14}C, and ^{3}H) to provide evidence on the recharge source of water and circulation dynamics of the Tangshan geothermal system near Nanjing, China. Tangquan hot spring group is located near Laoshan National Forest Park in the Pukou District of Nanjing, separated from the main urban area of Nanjing by the Yangtze River [23]. Li and Wang [24] have studied the water-bearing condition of natural mineral water No. 1 Springs between Anhui province and Laoshan Double springs of Xianxiang County in this area. Ding and Zhu [25] used geological analysis method to describe a conceptual model of regional scale groundwater flow for the thermal water proposed in the carbonate formation in Yeshan-Tangquan anticlinorium. According to the previous research results and exploration experience, hydrogeochemical and isotope methods are commonly used in detecting the groundwater circulation in this decade, but the results still need to be cooperated with the traditional geological analysis methods such as field investigation and geological exploration to analyze the geological formation elements of hot springs.

There are many karstic coldwater springs, low-temperature hot springs, and geothermal wells in the Weigang ore in the Lunshan area. The previous studies are all about Tangshan, Tangquan, and Xiangquan hot springs, but research on the origin of the Lunshan hot spring is still a blank. The studies on the origin of the hot springs focus on the water resource, pathway, and rising channels of the thermal groundwater, thermal reservoir, and cap rock. In

this article, the hot springs in the karst area around Nanjing are divided into two groups: Tangshan-Lunshan hot spring group and Tangquan-Xiangquan hot spring group. First, systematic hydrogeochemical and isotopic studies are carried out in Lunshan area, and schematic diagrams of the conceptual model of the geothermal water circulation in Lunshan based on the experimental results are plotted. Then, the connections and similarities of the four hot springs are discussed from a regional perspective in this study which were rarely mentioned in the previous studies. The discussion about the similarity of the origin of thermal groundwater is significant in improving the accuracy and efficiency of the exploration and development of geothermal resources in karst area around Nanjing.

1.1 Study area

The study area is located in the lower reaches of the Yangtze River, with geographical coordinates of 31°40′00″ to 32°20′00″ North and 117°30′00″ to 119°40′00″ East (Figure 1). The area has a subtropical monsoon climate with four distinctive seasons and abundant precipitation, and the climate in Nanjing is stable. The annual average temperature is 15.4°C, and the annual average amount of precipitation is 1,106 mm/annum with a long frost-free period and sufficient sunshine. The monthly average precipitation and temperature of Nanjing in 2010 are shown in Figure 2.

The study area is located in the middle and lower reaches of the Yangtze Plain. The Yangtze River runs through the study area from southwest toward east and divides the area into two parts (the northern part and the southern part). There are four groups of hot springs in the study area, and depending on the hydrogeological characteristics of the distribution of the hot springs, it can be divided into two major areas: The Tangshan-Lunshan anticlinorium area and the Tangquan-Xiangquan anticlinorium area. The Tangshan hot spring group is located at the foot of the Tangshan Mountain in the Tangshan-Lunshan anticlinorium of the Ningzhen Mountains in

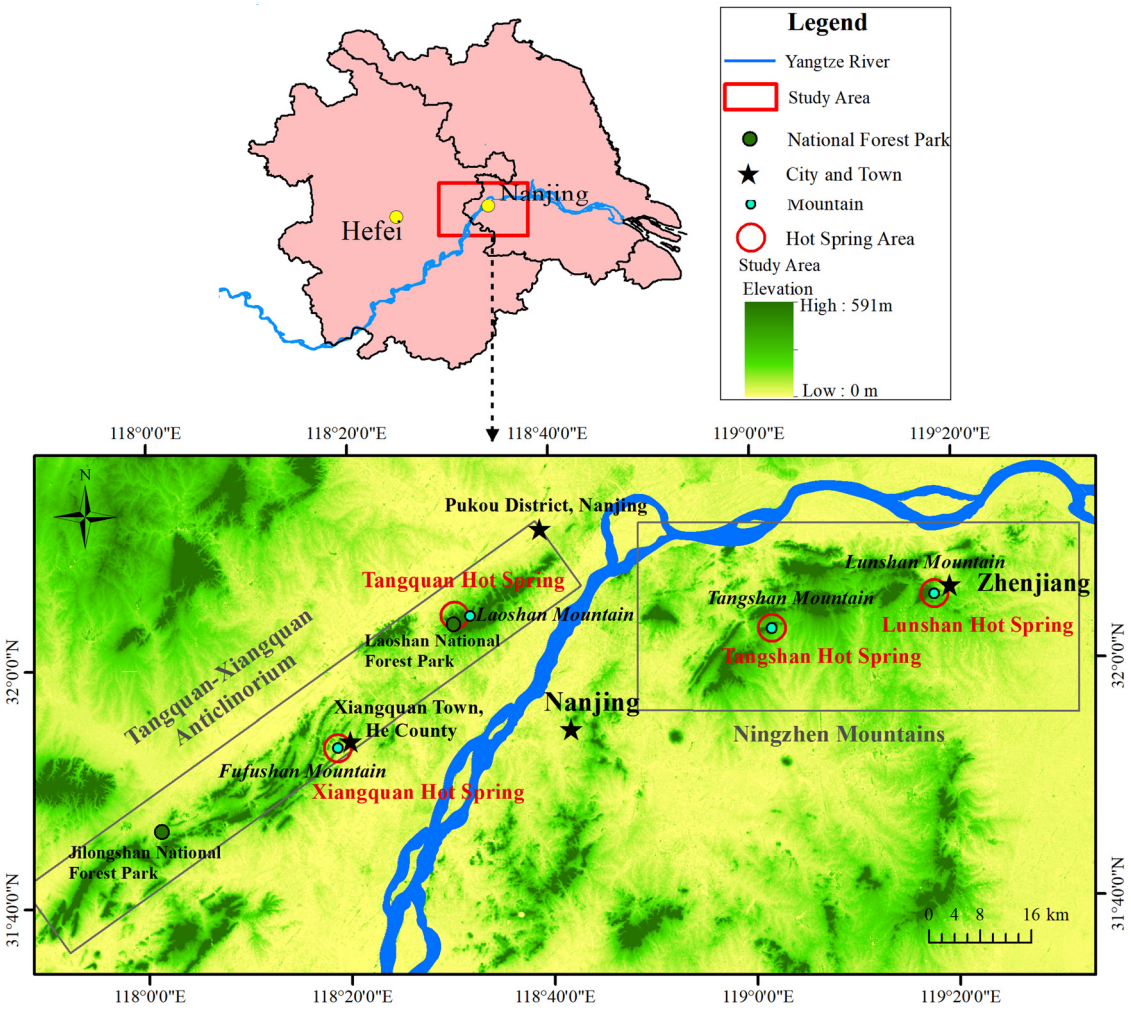

Figure 1: Geographical location of the study area.

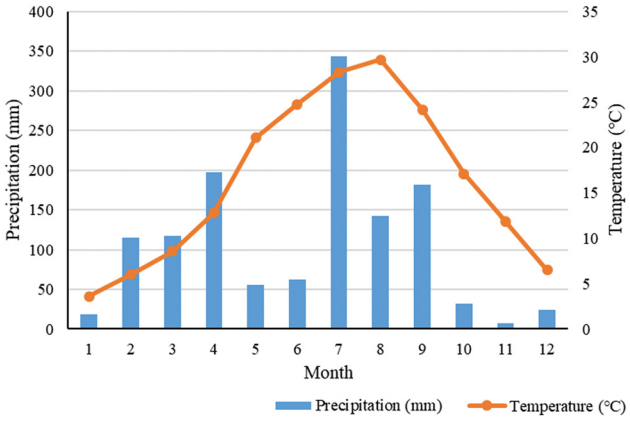

Figure 2: The monthly average precipitation and temperature of Nanjing in 2010.

the southeast of the study area, and Lunshan hot spring group is located at the foot of Lunshan Mountain in Zhenjiang. The low-temperature hot springs are located on the west side of Lunshan Mountain with low development and utilization and are currently used only for aquaculture. Geothermal water was drilled from a well in the Weigang iron ore in the 1970s, and a comprehensive fitness and leisure location with hot springs was then established. Overall, the Tangquan hot spring group and the Xiangquan hot spring group are located in the Tangquan-Xiangquan anticlinorium, in the northwest of the study area across the Yangtze River from Ningzhen Mountain area. Tangquan hot spring group is located in the Tangquan Town near Laoshan National Forest Park in Pukou District of Nanjing. There are three famous springs in the Laoshan scenic spot, among which Pearl spring and Amber spring are located at the east end of Laoshan Mountain. At the same time, there are hot springs distributed in a belt ten miles long in the Tangquan area, which are located in the southwest of the Laoshan Mountain. Hot springs are exposed at the foot of Fufu Hill around Jilongshan National Forest Park. Xiangquan hot springs are located in Xiangquan Town of He County, Anhui province, and 16 geothermal wells are used for hot spring baths and breeding in Xiangquan Town of He County in the southwestern part of the study area.

2 Materials and methods

2.1 Analysis of geological condition

As a relatively independent hydrogeological unit, the thermal water circulation system needs groundwater recharge, runoff, and drainage conditions. In the research on the origin of the four hot spring groups, analysis of geological conditions is important. Field perambulation, survey, and information collection are carried out. In the southeastern part of the study area, the Ningzhen Mountain range is a slightly east-west-north arc-shaped mountain range and stretches for 100 km. The strata of Ningzhen Mountains are mainly composed of Sinian to Triassic rocks. After a long period of weathering, erosion, and fault activity, accompanied by multiple intrusions and extrusions of igneous rocks, a broken chain of mountains was finally formed [26]. The Tangshan-Lunshan anticlinorium which is located in the southern Ningzhen uplift structure, is less affected by fractures and magmatic rocks (Figure 3). It is the clearest arc fold in this area, with a total length of approximately 60 km and a maximum width of 9 km. The Tangshan short-axis anticline is located in the core of the Tangshan-Lunshan anticlinorium. The elevation of Tuanzijian, the main peak of Tangshan, is 241 m. The main trend of Tangshan is nearly E–W, and the fault structure is complex, including the E–W main fault, N–SW–E translation fault, and NE fault. The exposed strata in the Tangshan area are from Paleozoic to Cenozoic in age, and the main soluble rocks are Cambrian and Ordovician carbonate rocks, including limestone, dolomite, calcareous dolomite, and dolomitic limestone. Karst caves of different sizes are widely distributed through the expansion and connection of dissolution fissures, and many karst landforms such as clint, dissolved ditch, and funnel are developed [26,27]. The insoluble rocks (mainly including the Silurian, Devonian, and Cretaceous sedimentary rocks) are distributed in the periphery of the Tangshan. The axis of Lunshan Mountain in the Tangshan-Lunshan anticlinorium is NE, and the core of the anticline is composed of Sinian dolomite. Upper Paleozoic strata are located in the two limbs of the Lunshan Mountain. The strata in the northwest limb and at the northeast end of Lunshan Mountain are cut off by faults and partially damaged, and granite is distributed at the east end. The direction of the fold axis in this area is NE–E to SW–W. The karst caves and dissolution phenomena are developed in dolomite, limestone, and marble along the fault zone and form a dissolution fracture zone, containing rich karst fracture water. In the north limb of Lunshan Mountain and south piedmont of Lunshan, most of the cold karst springs are distributed along the water separation boundary and structural fault zone, and the karst fracture water in other areas is covered by volcanic rock and the Quaternary system.

In the western part of the study area, the Tangquan-Xiangquan anticlinorium follows a trend from southwest-northeast. Laoshan National Forest Park is located in the northeastern area of the anticline structure. There are

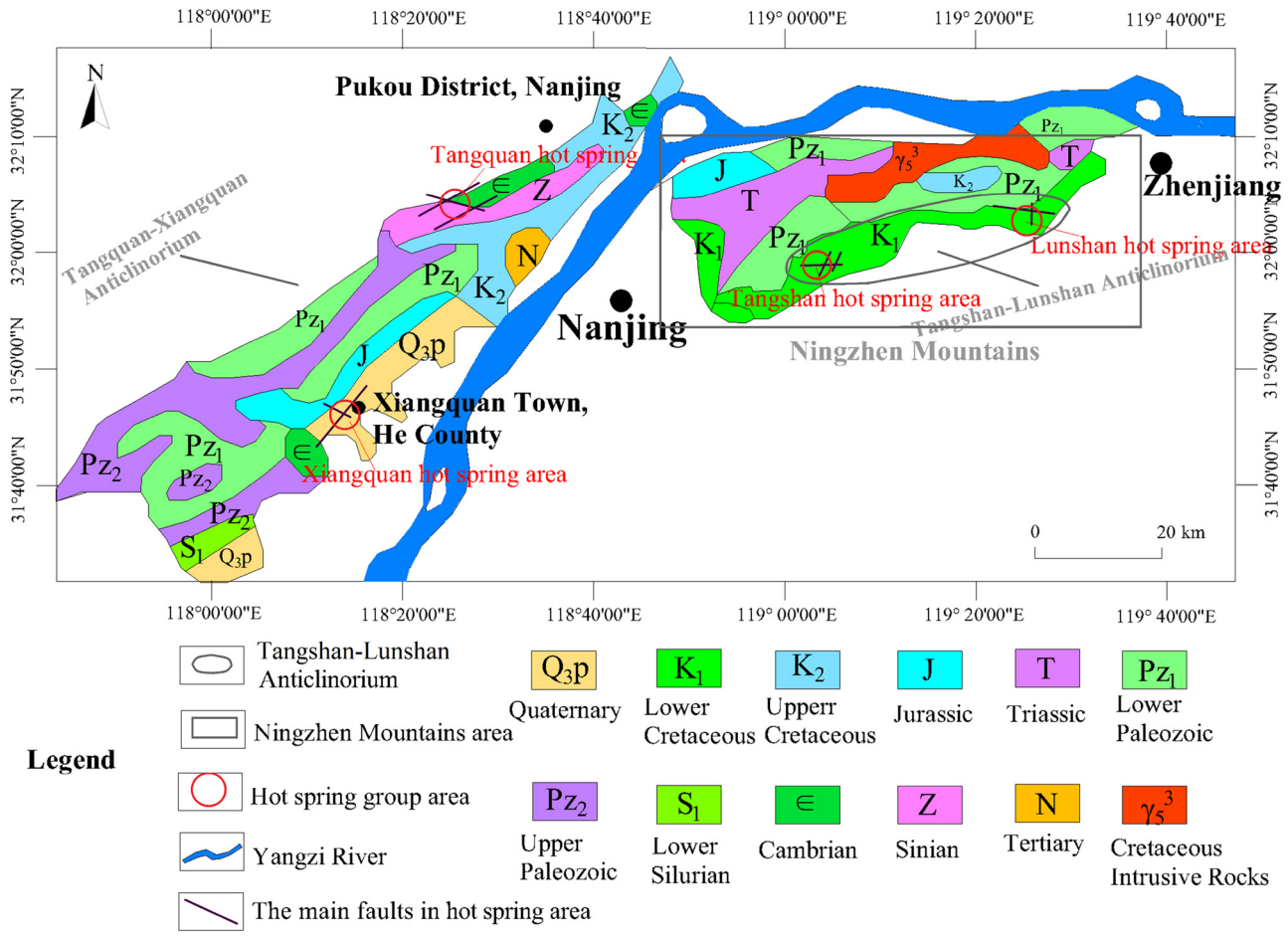

Figure 3: Geological map of the Ningzhen Mountains and Tangquan-Xiangquan anticlinorium (1:5,000,000).

nearly 100 mountains and small peaks, and Longdong Mountain, with an elevation of 442 m, is the highest mountain in this area. The mountain is mainly composed of Sinian limestone, Sinian phyllite, Cambrian limestone, Cretaceous sandstone, etc., with well-developed limestone caves and abundant karst fissure groundwater. Jilongshan National Forest Park in the southwestern part of the Tangquan-Xiangquan anticlinorium is located in He County, Anhui province, and belongs to the lower Yangtze stratum [18]. The Laoshan Mountain range follows a southwest-northeast trend, and elevation of the main peak is 275 m. The exposed bedrock is widely distributed in this area, which forms a hilly area with an "S" shape in the northeast direction. The Tianfan piedmont with Quaternary cover is distributed in the northwestern corner and both sides of the middle ditch, and magmatic rocks are not well developed. There is a series of NE and NW faults in this area, and the main fold is a syncline with an axial direction of N25°-50°. The fault structure is well-developed in the northeast direction [26]. The hot springs and geothermal wells are distributed at the northwestern foot of Fufu Mountain, and the Ordovician siliceous limestone is distributed in the core area of the Longwangshan anticline. The siliceous limestone can be easily broken, especially after being stressed in the core of the anticline. The effect of groundwater flow causes fissure karst caves to develop, which are good channels for the migration and storage of groundwater and geothermal water [27].

The main thermal control structures are the basin-margin fault step belt, the southern Jiangsu uplift of the internal Indosinian surface of the basin, and the favorable fold structure in the uplift area. The geothermal gradient is generally less than 2.5°C/100 m [18,28].

2.2 Collection of samples and analysis of hydrogeochemical data

Hydrogeochemical and isotope methods were used to describe the characters of Lunshan hot spring. The sampling was carried out by Huadong Engineering Corporation Limited, China and Hohai University on October 9th, 2010,

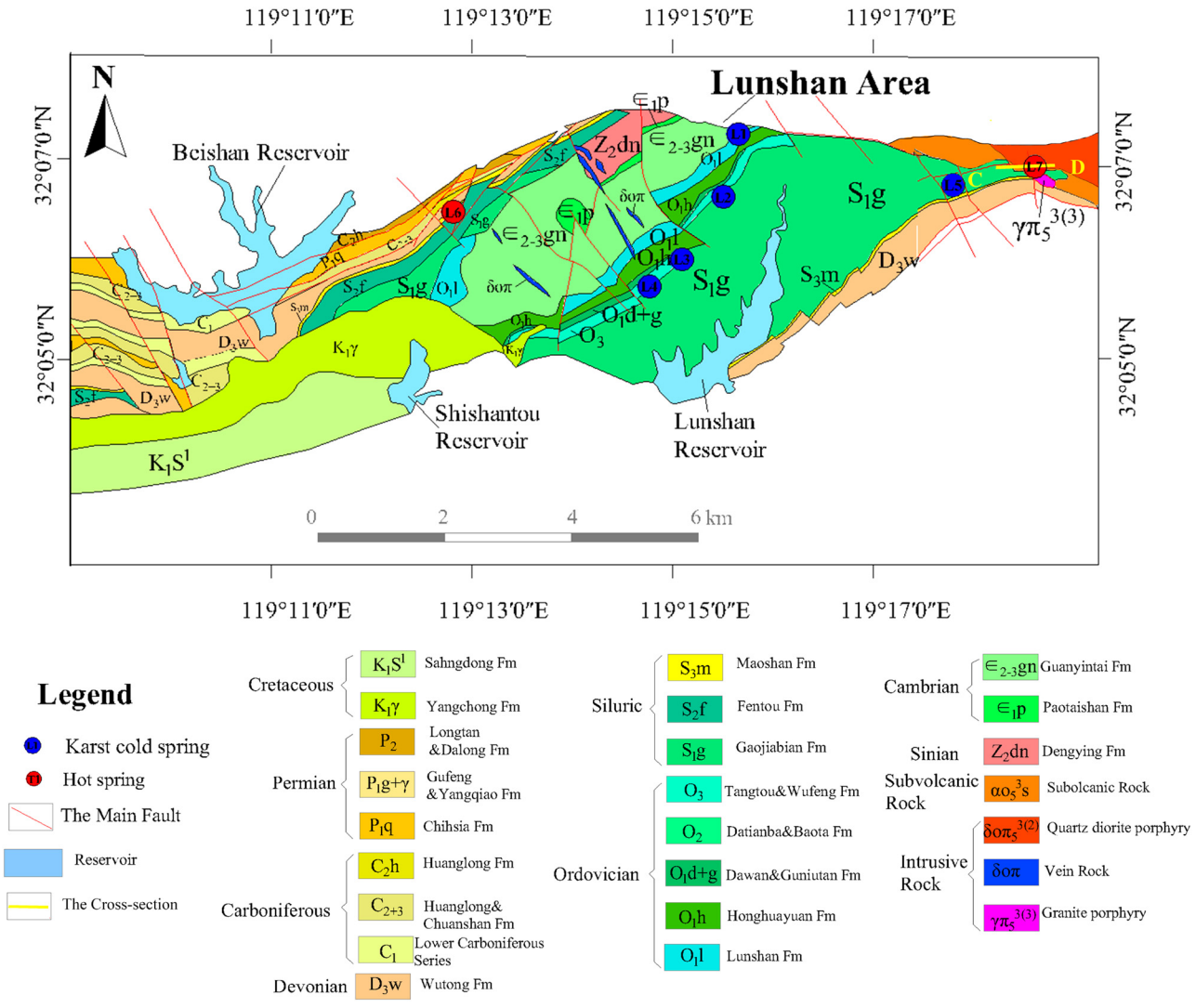

Figure 4: Geological map and distribution of karst springs in the Lunshan area in the Ningzhen Mountains.

and the sampling points are indicated in Figure 4. There are seven samples in the Lunshan area, including five cold karst groundwater samples (L1–L5) and two geothermal water samples (L6 and L7). The water surface elevation and groundwater temperature of the sampling points were collected at the same time (Table 1). The temperature of hot spring L6 at Yaolinkou pig farm is 25°C, which is a low-temperature hot spring, and it is used to breed duckweed and fish. L7 is the geothermal water in the Weigang ore. Water temperature, pH, electrical conductivity, and water flow rate were measured in the field. Samples for major element chemistry were filtered and collected in 50 mL high-density polyethylene bottles with a 0.45 µm filter. Five samples were collected in 50 mL glass bottles and analyzed for $\delta^{18}O$, δD, and ^{3}H compositions at laboratories of Huadong Engineering Corporation Limited, China. Geochemical and isotopic analyses were performed in the laboratories of Huadong Engineering Corporation Limited, China within about 1 week after collection, and the results were precise.

Table 1: Water surface elevation and water temperature of the sampling points in Lunshan area (October 9th, 2010)

Sample ID	Water surface elevation (m)	Water temperature (°C)	pH	EC (mS/cm)	Water flow rate (L/s)
L1	75.00	16.90	6.70	0.45	3.50
L2	78.00	20.10	6.58	0.52	2.70
L3	77.00	—	—	—	20.79
L4	78.00	—	—	—	1.19
L5	52.00	20.80	6.69	0.39	1.5
L6	60.00	25.00	—	—	—
L7	—	49.00	—	—	—

Table 2: Hydrogeochemical analysis results of karst groundwater samples in Lunshan

Sample ID	Cation content (mg/L)				Anion content (mg/L)			Total salinity (mg/L)	H_2SiO_3 (mg/L)	Hydro-chemical type
	Ca^{2+}	Mg^{2+}	Na^+	K^+	HCO_3^-	Cl^-	SO_4^{2-}			
L1	80.20	35.80	2.79	0.30	367.00	11.20	25.50	531.00	10.60	HCO_3–Ca–Mg
L2	86.90	41.00	4.26	0.30	363.00	15.00	43.60	565.00	14.20	HCO_3–Ca–Mg
L3	84.30	37.00	3.20	0.34	343.00	12.70	46.40	536.00	11.80	HCO_3–Ca–Mg
L4	86.00	33.40	3.10	0.28	359.00	9.72	35.80	538.00	14.00	HCO_3–Ca–Mg
L5	93.00	6.48	5.88	0.34	237.00	11.20	53.20	424.00	21.30	HCO_3–Ca
L6	69.00	33.40	3.28	0.37	308.00	7.48	26.00	457.00	12.30	HCO_3–Ca–Mg
L7	420.00	52.00	25.60	14.40	160.00	15.00	1171.00	1923.00	84.40	SO_4–Ca

3 Results

The hydrogeochemical analysis results are shown in Table 2. The isotopic analysis was carried out for five springs, including four cold karst groundwater samples and one geothermal water sample as shown in Table 3.

The Piper plot of all water samples (Figure 5) is drawn according to the results in Table 2. Based on the results of the hydrogeochemical analysis, there are three hydrogeochemical types of groundwater in the study area. HCO_3–Ca–Mg type groundwater is mainly distributed in the area composed of dolomite and dolomitic limestone aquifers on Lunshan Mountain, and the water quality type is characterized by high Mg^{2+} content. HCO_3–Ca type water is mainly distributed in the hydrogeological unit dominated by the lower limestone reservoir. Weigang ore thermal water sample L7 is SO_4–Ca type. The calcium ion contents of the L1–L6 groundwater samples are approximately 80–90 mg/L, and the magnesium ion contents of the groundwater samples in the dolomite area are 30–40 mg/L, while that in the limestone area are less than 10 mg/L. In contrast, the content of sodium in groundwater is slightly lower in the dolomite area, while that in the limestone area is slightly higher. The anionic content and H_2SiO_3 content of water samples have little difference, and the mineralization degree shows little change. The cation content in the Weigang ore thermal water is generally higher, the main anion is SO_4 (1171.00 mg/L), and the H_2SiO_3 content is high (84.40 mg/L), which is related to deep hydrogeological conditions.

The isotopic results show that δD can be divided into three types (Figures 6 and 7): L1–L3 cold karst springs in the northeast of Lunshan ranges from −50.0 to −51.1‰, and the lowest value of L7 Weigang ore thermal water is −55.5‰, while the spring near L7 Weigang ore geothermal water is −43.3‰. $\delta^{18}O$ can be divided into three types: $\delta^{18}O$ of L1 Xianshuiyan spring water sample and L7 Weigang ore thermal water sample are from −8.61 to −8.63‰, $\delta^{18}O$ of L2 Laohutou spring and L3 Xianrendong spring, which are located in the south slope of Lunshan, are from −7.32 to −7.33‰, $\delta^{18}O$ of L5 Jiupin Quarry spring is −5.81‰. The ^3H (TU) of cold spring water samples are 3.60–4.83‰, and the thermal water sample in

Table 3: Isotopic analysis results of karst groundwater samples in Lunshan

Sample ID	δD	$\delta^{18}O$	^3H		$d = \delta D - 8 \times \delta^{18}O$
			Bq	TU	
L1	−51.1	−8.63	0.43	3.68	17.94
L2	−50.0	−7.32	0.57	4.83	8.56
L3	−50.6	−7.33	0.44	3.72	8.04
L5	−43.3	−5.81	0.43	3.60	3.18
L7	−55.5	−8.61	0.21	1.76	13.38

Note: δD < 1‰ and $\delta^{18}O$ < 0.1‰.

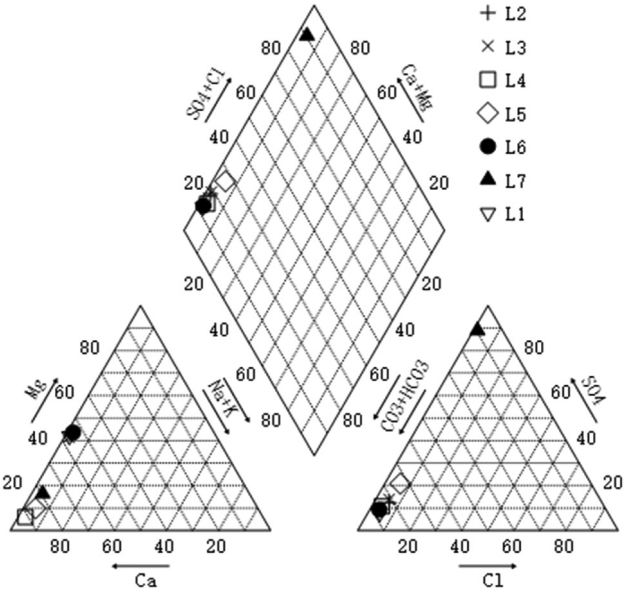

Figure 5: Piper plot of all water samples in the Lunshan area.

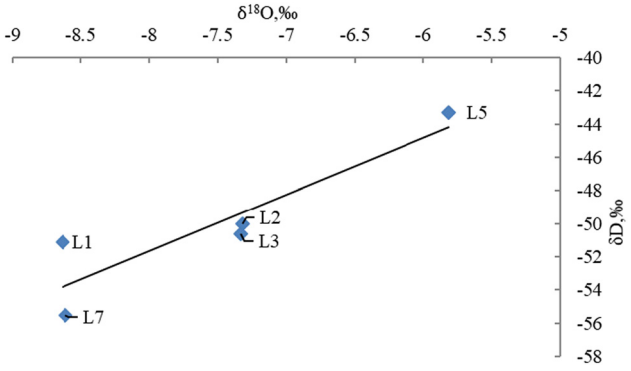

Figure 6: Distribution diagram of $\delta D \sim \delta^{18}O$.

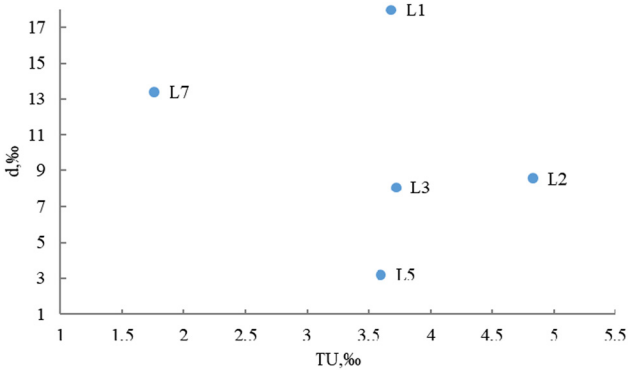

Figure 7: Distribution diagram of d~TU.

Weigang ore is only 1.76‰. The deuterium (D) excess parameter d ($d = \delta D - 8 \times \delta^{18}O$) of the samples are dispersed in Figure 6, which shows that the groundwater is replenished by atmospheric precipitation but has different properties through different groundwater circulation processes.

4 Discussion

4.1 Lunshan hot spring

4.1.1 Water–rock reaction in Lunshan area

Water–rock reactions are important geochemical processes in geothermal water and shape the characteristics of water chemistry [12]. The linear relationship between mNa and mCl (as mmol/L) is shown in Figure 8a. The relationship between m(Ca + Mg) and $m\mathrm{HCO_3}$ (as mmol/L) is given in Figure 8b, between mCa and mMg (as meq/L) is given in Figure 8c, and between mCa and $m\mathrm{SO_4}$ (as meq/L) is given in Figure 8d.

Some cold groundwater samples plot near the line of mNa:mCl = 1:1, suggesting that Na and Cl were mainly derived from NaCl dissolution [29]; however, the geothermal groundwater samples lie below the line of mNa:mCl = 1:1, indicating that apart from NaCl dissolution, dissolution of albite in the formations (equation (1)) might contribute to the additional Na [29]:

$$2\mathrm{NaAlSi_3O_8} + 9\mathrm{H_2O} + 2\mathrm{H_2CO_3} \rightarrow \mathrm{Al_2Si_2O_5(OH)_4} + 2\mathrm{Na^+} + 2\mathrm{HCO_3^-} + 4\mathrm{H_4SiO_4} \quad (1)$$

The geothermal groundwater sample lies above the line of m(Ca + Mg):$m\mathrm{HCO_3}$ = 1:1, while the cold groundwater samples are plotted below the line (Figure 8b). All samples lie above the line of mCa:mMg = 1:1, and the ratios of mCa to mMg are much greater in geothermal groundwater samples (Figure 8c). Geothermal groundwater sample is plotted below the line of mCa:$m\mathrm{SO_4}$ = 1:1, while all cold groundwater samples lie above the line (Figure 8d). The different characteristics of the chemical compositions suggest different water–rock interaction processes and weak connections between the cold groundwater and the geothermal groundwater. If dissolution of only calcite and dolomite (equations (3) and (4)) occurred in the geothermal reservoir, the ratio of m(Ca + Mg) to $m\mathrm{HCO_3}$ should be <1 [29,30]. The high content of Ca and $\mathrm{SO_4}$ and the ratio of mCa to $m\mathrm{SO_4}$ of the geothermal groundwater close to 1 in this study suggest that except for carbonate dissolution, anhydrite (embedded in carbonate rock) dissolution (equation (2)) also occurred and it dominates the water–rock interaction processes in the geothermal reservoir [31]. The geothermal groundwater sample lying below the line of mCa:$m\mathrm{SO_4}$ = 1:1 (Figure 8d) is because of the significant dissolution of gypsum which may lead to the precipitation of carbonate minerals to some extent.

Anhydrite dissolution = precipitation:

$$\mathrm{CaSO_4} \leftrightarrow \mathrm{Ca^{2+}} + \mathrm{SO_4^{2-}}, \quad (2)$$

Calcite dissolution = precipitation:

$$\mathrm{CaCO_3} + \mathrm{H_2O} + \mathrm{CO_2} \leftrightarrow \mathrm{Ca^{2+}} + 2\mathrm{HCO_3^-}, \quad (3)$$

Dolomite dissolution = precipitation:

$$\mathrm{CaMg(CO_3)_2} + 2\mathrm{CO_2} + 2\mathrm{H_2O} \leftrightarrow \mathrm{Ca^{2+}} + \mathrm{Mg^{2+}} + 4\mathrm{HCO_3^-}. \quad (4)$$

The ^{3}H (TU) results show that the age of cold groundwater samples are younger than the thermal groundwater sample, and the thermal groundwater go through deeper circulation processes.

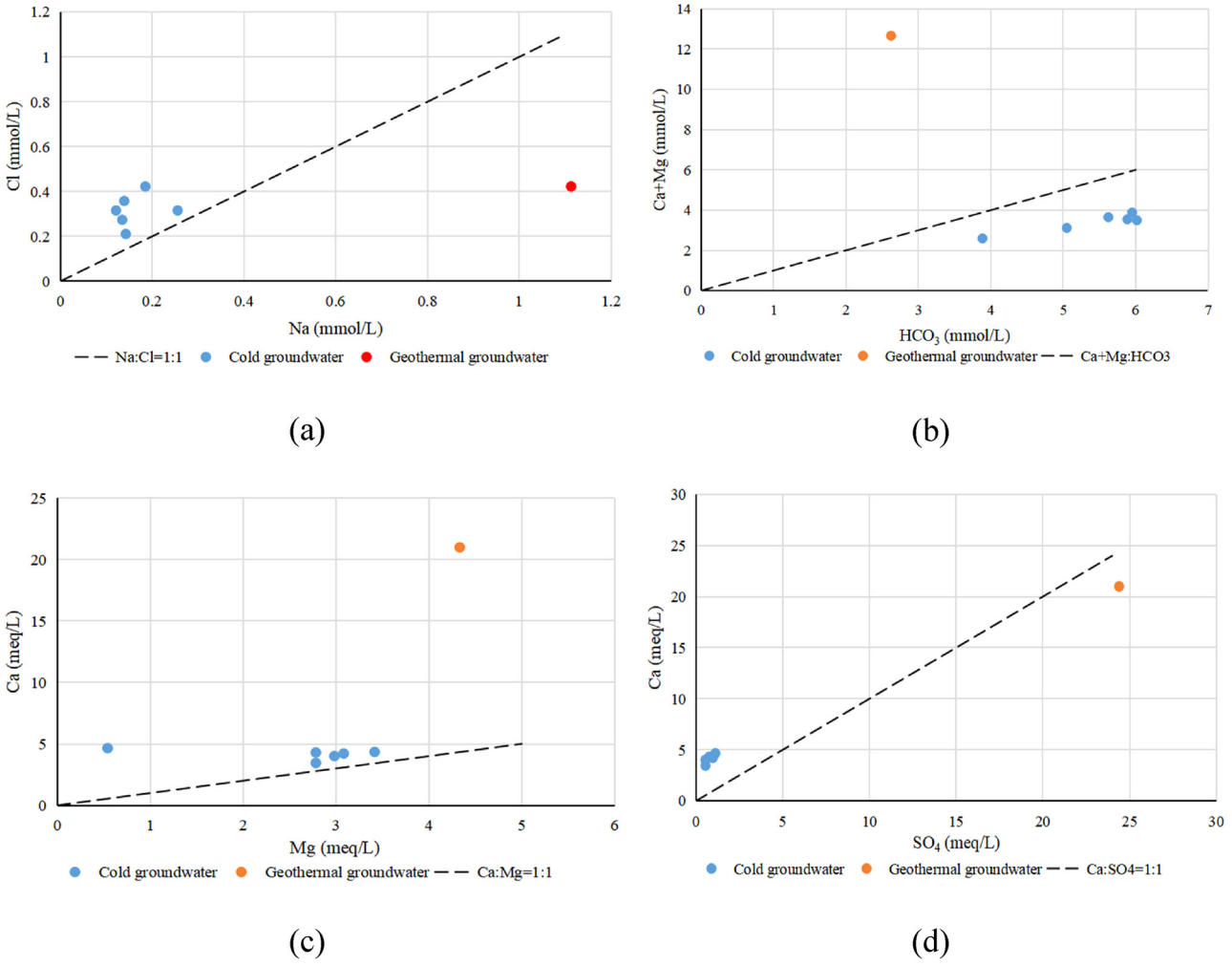

Figure 8: Major ion ratio relation: (a) Na–Cl; (b) Ca + Mg–HCO_3; (c) Ca–Mg; (d) Ca–SO_4 of geothermal groundwater and cold groundwater samples.

4.1.2 The conceptual model of geothermal water circulation in Lunshan area

Karst phenomena are common and strong at the intersections of faults in the Lunshan area. The shallow karst is mainly filled with paleokarst caves and karst gaps, and the deep karst is mainly controlled by the regional faults and the distribution of pyrite, but the development of deep karst is weak in general with no connected underground karst pipeline, underground rivers, or other large-scale karst forms. The local groundwater is mainly recharged by precipitation, and the development of karst is conducive to the migration of groundwater. Through different groundwater circulation processes, cold karst water exposed along the faults becomes cold springs or further joins the deep circulation and is heated to become geothermal water, rising along the faults or discharging through the geothermal wells under specific reservoir and cap rock conditions.

The karst fissure water is mainly distributed in the Lunshan area. Precipitation infiltration recharges the groundwater, and the groundwater runoff around the piedmont gradually leads to the convergence of the water catchment fault, and finally erodes and overflows into springs near the lithologic boundary; the L2, L3, and L4 springs all belong to this category. Although the formation containing springs L1 and L5 on the northern slope of Lunshan Mountain has a reverse dip structure, under the condition of a topographic catchment, groundwater discharges to the piedmont runoff along the dissolution fissures, and springs are exposed due to the fault blocks.

In the north of the Weigang ore area, the groundwater level of the thermal well is 18 m. With the development of underground mining and tunnels, the cold

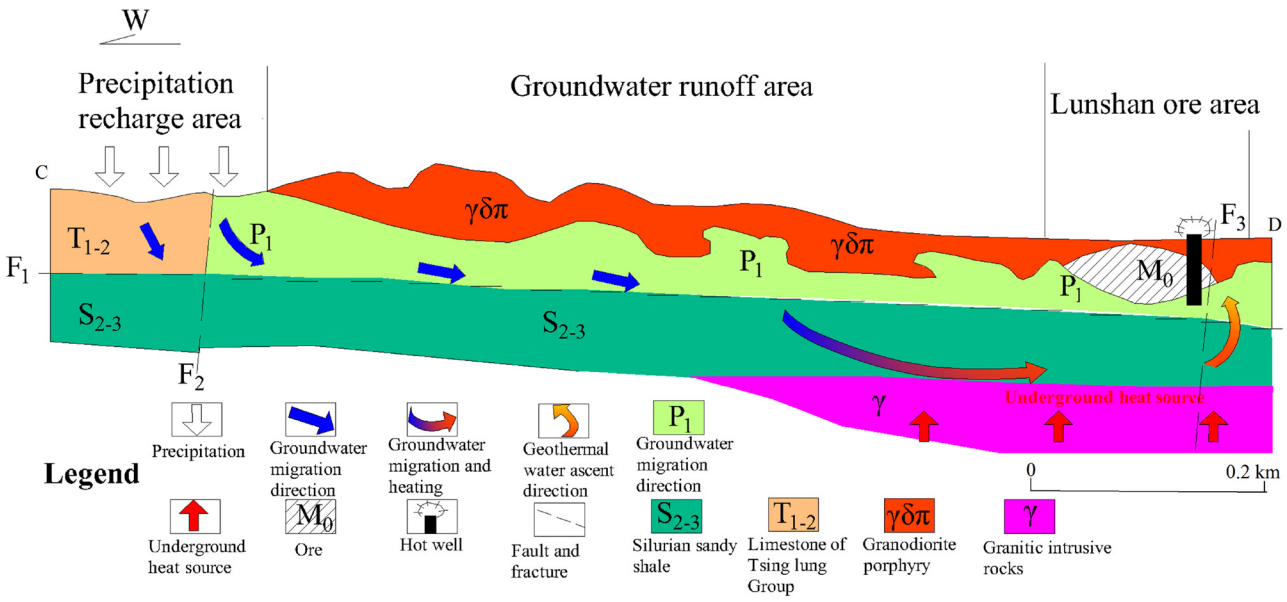

Figure 9: Conceptual model of geothermal water circulation process in the Weigang ore of Lunshan area (cross-section C and D in Figure 4).

groundwater level continues to decrease, and the surface water gushing is cutoff as well. Due to the insufficient recharge of cold water and the decrease in water volume, the temperature of hot water gradually increases from 45 to 49°C, and hot water becomes the main fraction of the underground water in Weigang ore area.

Weigang ore thermal water is formed by deep groundwater circulation along the NW and SN faults, which has little influence on the activity of the shallow groundwater. In the northern strip of the mountains, 4–5 km away from the Weigang ore area, the Qixia limestone of the Permian system in the hanging wall of the F_2 fault (Figure 9) is widely exposed, with an elevation of more than 80 m higher than that in the ore area, and dissolution phenomena are developed. In this area, groundwater receives recharge from atmospheric rainfall. According to the analysis of the water inflow, water inflow characteristics and water quality in the pit, it is believed that the pit water in the Weigang ore is supplied by the infiltration of atmospheric precipitation through the eastern Lunshan Reservoir. Because the shallow part is mainly covered by intrusive rock masses, the cold groundwater is forced to enter the deeper circulation along the Weigang fault (F_1), and it is heated by a geothermal gradient or hydrolysis of sulfide minerals such as pyrite. The hot water in fractured rock has strong dissolution ability, and fissures, small karst caves, and broken cores have developed in this area. The hot water in the structural fault in the ore area trends N60°W (F_3), with a dip angle close to vertical; it cuts through the deep granodiorite porphyry, and its top penetrates a complete marble. The marble forms a semipermeable cover between the hot water fault and the upper cold water fault, which is the main channel for hot water that fills in the ore area. In the hot water fault zone of the Yanshanian granodiorite porphyry underlying the mine, the fault cuts through the orebody, skarn, and marble; it is a new structural fault. In general, the underground water of the Lunshan Mountain circulates to the east along the strike of the Qixia limestone in the Weigang fault and enters the deep circulation blocked by the rock mass. After heating, the thermal water rises along the fault, and is drained through the mine pit.

4.2 Summary of the genesis of Tangshan, Tangquan, and Xiangquan hot springs

The genesis of the Tangshan hot spring is similar to the Lunshan hot spring, and they all are distributed in the Tangshan-Lunshan anticlinorium. Through field investigation and data collection, six karst geothermal water wells in Tangshan are plotted in Figure 10. The thermal reservoir is Cambrian-Ordovician rock strata, and the water quality is SO_4–Ca–type [18]. Lu et al. [12] indicated that the local precipitation in the Cambrian and Ordovician carbonate areas is the source of geothermal water, and the geothermal water runoff in the Tangshan area involves mainly the flow of karst fissure water in the

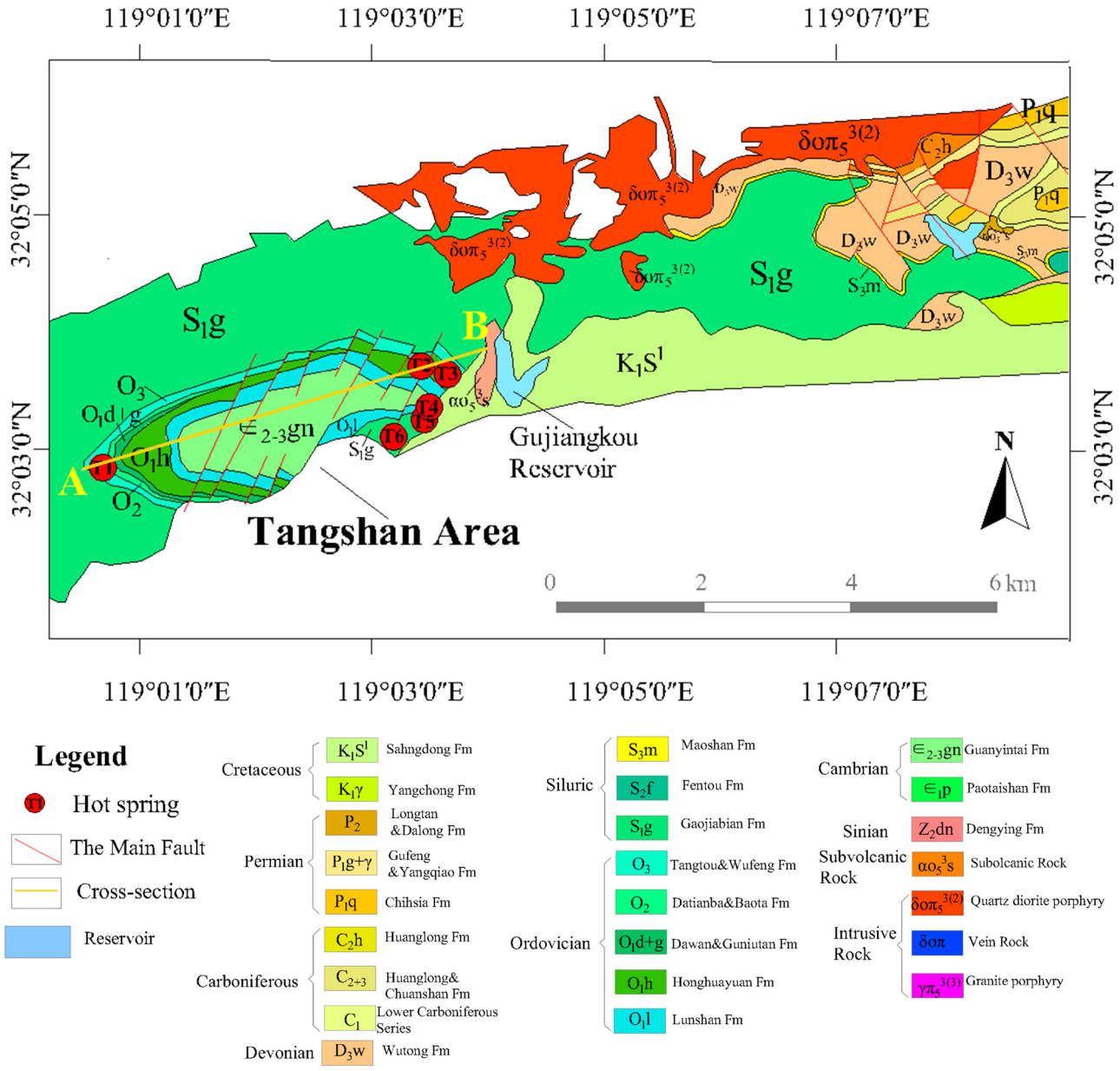

Figure 10: Geological map and distribution of karst springs in the Tangshan area in the Ningzhen mountains.

carbonate fissure cave spaces. In the Tangshan area, most of the strata are oriented from SW to NE (Figure 3), and fissures are developed. The direction of groundwater flow is also from SW to NE, and when tensile fissures are perpendicular to the strike of the strata, the direction of groundwater flow is changed to from NW to SE [19]. At the same time, the groundwater is heated gradually in the process of deep circulation, and the dissolution of carbonate and gypsum mainly occurs in the runoff process. The temperature of the deep geothermal water is 87°C, and the depth of the groundwater circulation is approximately 2.5 km, but during the upwelling process, the temperature of the geothermal water is reduced by 63% due to mixing with cold water [12].

The karst thermal reservoir is distributed through the Tangshan hot spring area. According to the theory and calculation of the "low-medium temperature convective geothermal system" [32], the heat source in the Tangshan area is the heat from the shallow crust to the deep crust, and there is no additional heat source. The cross-section of the Tangshan anticline presents this ridge type with a wide bottom and narrow top, which is conducive to the refraction and redistribution of heat flow. Therefore, the Earth's heat flow in the limb of the Tangshan anticline

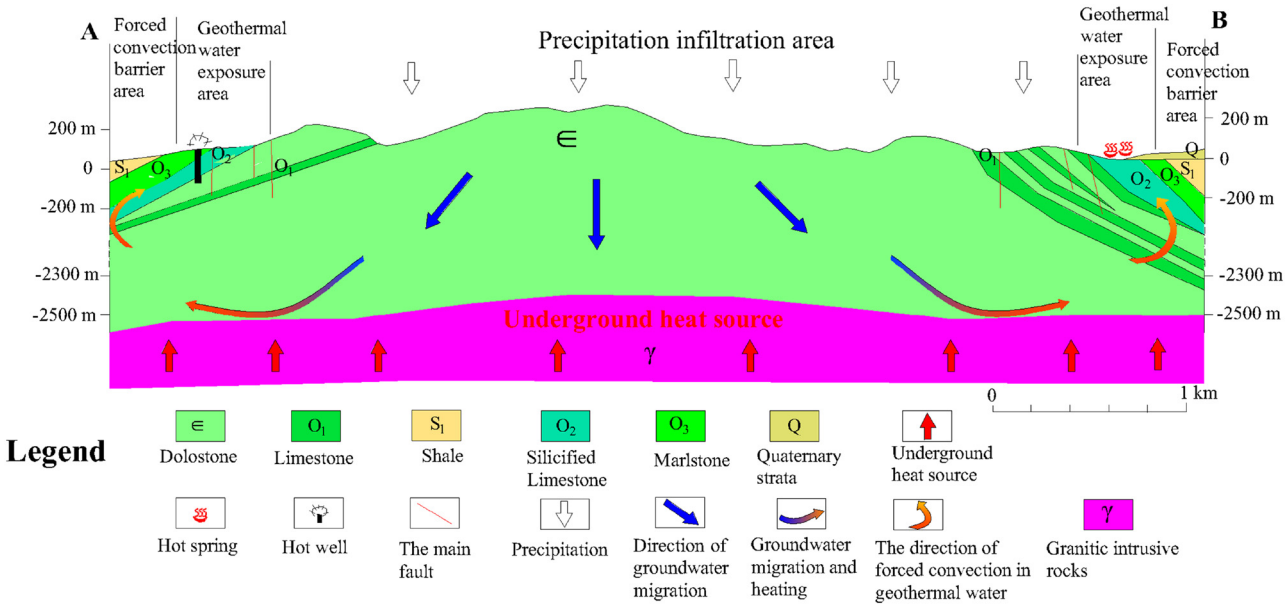

Figure 11: Conceptual model of geothermal water circulation process in the Tangshan hot spring group (cross-section A and B in Figure 10) (enriched and plotted based on Figure 2 in "The type of low-medium temperature geothermal system of convection type, the genesis analysis of Tangshan geothermal system in Nanjing" [19]).

can converge to the axis, resulting in a relatively high heat flow value in the ridge area along the axis of the anticline [33].

In the flank area of the Tangshan anticline, Silurian shale is the main rock. This lithology is conducive to blocking the infiltration of peripheral groundwater into the axis of the anticline, preventing heat loss and providing good insulation; moreover, this lithology and structure prevent excessive migration and diffusion of deep geothermal water to the outside in the process of circulation, which are conducive to the occurrence of deep hot water. The faults in the Silurian shale strata are not developed. At the same time, due to the poor permeability, low thermal conductivity, and high thermal resistance of shale, it has also become an aquifer roof with good heat insulation, water resistance, and heat preservation effects [21]. The Tangshan hot spring is mainly exposed at the intersection of two groups of NE and EW trending faults, showing a NE zonal distribution, which can be considered a group of thermal water control faults [12,19]. The conceptual model of groundwater circulation process in the Tangshan hot spring area is shown in Figure 11.

The previous studies indicated that the origin of Tangquan and Xiangquan hot springs are very similar to Tangshan and Lunshan hot springs. The hot spring water of Tangquan is SO_4–Ca type or SO_4–Ca–Mg type at 30–42°C, and is mainly infiltrated by atmospheric precipitation [18,25]. Faults and folds are developed in the area, mainly in the NE and NW directions, and the strike angle of the lower Cambrian sandy shale and carbonaceous shale of the main mountains in the area are not integrated into the upper Sinian calcareous dolomite (Figure 3). In addition, due to the influence of structural movements, the dolomite is hard, brittle, and easily broken, thus fractures and karst caves have developed, which are conducive to the infiltration of precipitation into the deep circulation, which is then heated by the underground heat and hydrolysis heating of sulfide minerals to become thermal water [25]. Shale is the cap rock, and the hidden fault in front of the mountain is the hot water drainage channel through which the spring water is discharged [24]. It has become a convective geothermal resource in the uplifted mountain area, and forms a karst thermal reservoir.

In the Xiangquan area, the thermal water temperature is 46–47°C, the thermal water type is SO_4–Ca–Mg, and the thermal water source is mainly recharged by atmospheric precipitation infiltration [18,25]. The siliceous limestone and limestone section of the Upper Ordovician Tangtou Formation in the core of the anticline is broken, and fissure karst caves have developed. Atmospheric precipitation enters the deep circulation through fractures and karst caves and is heated by an underground heat source. The Silurian mudstone, sandstone, and shale on both sides of the anticline are cap rocks for geothermal water. Geothermal wells and hot springs are

Table 4: The characters of the hot spring groups around Nanjing

Characters	Tangshan hot spring group	Lunshan hot spring group	Tangquan hot spring group	Xiangquan hot spring group
Geological division	Tangshan-Lunshan anticlinorium		Tangquan-Xiangquan anticlinorium	
Karst landform	Developed in the piedmont area	Developed in fault intersection area	Developed in the piedmont area	Developed in the core of anticline
Thermal water type	SO_4–Ca	SO_4–Ca	SO_4–Ca/SO_4–Ca–Mg	SO_4–Ca/SO_4–Ca–Mg
Water source	Infiltration of atmospheric precipitation	Infiltration of atmospheric precipitation	Infiltration of atmospheric precipitation	Infiltration of atmospheric precipitation
Water temperature	25–60°C	45–49°C	30–42°C	46–47°C
Heat source	Geothermal heating	Geothermal heating	Geothermal heating and hydrolysis heating of sulfide minerals	Geothermal heating
Thermal reservoir	Cambrian-Ordovician limestone	Cambrian-Ordovician limestone	Sinian limestone	Ordovician limestone
Cap rock	Shale	Granodiorite porphyry and marble	Shale	Shale and sandstone
Channel for thermal water ascent	Intersection of NE fault and EW fault	NW and SN fault	NE and NW faults	NE and NW faults

located in the structure that cuts near the EW transverse fault, and a water storage structure is formed with the NE fault and then extends to the NW, that is, the intersection with the regional NW fault (Figure 3), forming a channel for the ascent of deep thermal water. After convection and heating, a fluid density difference is generated, which superimposes the driving force of thermal diffusion, making the geothermal water migrate along the structural channel and exposing it to form hot springs [25]. Therefore, the Xiangquan hot spring area is a convective hot spring resource in the uplifted mountainous area, deeply affected by the dome fault-fold belt, and controlled by the NE fault.

5 Conclusion

The origin of hot springs are site depending on the survey and analysis results, which show that the characters of the 4 hot spring groups in the karst landform around Nanjing are very similar. The characters are summarized in Table 4. The similarities of the origin of the hot springs around Nanjing are as follows: (1) The four hot springs are all low-medium temperature hot springs with temperatures below 60°C, and the spring water types are SO_4–Ca or SO_4–Ca–Mg in the karst landform area. (2) The hot springs are mostly present near the core of the anticlinal structure of karst strata, mainly distributed in the Ordovician, Cambrian, and Sinian limestone strata, with volcanic rocks and intrusive rocks. (3) Most of the groundwater supply sources are from local atmospheric precipitation, and infiltration of precipitation recharges the groundwater sources from the anticlinal structure, forming local groundwater deep circulation in the spring domain and obtaining heat from the ground. (4) At the intersection of the two groups of fault zones, channels for the ascent of geothermal water form more easily, and the four convective hot spring groups are distributed along the fault zone of the anticline structure.

In general, the pit water in the Weigang ore of Lunshan area is supplied by the infiltration of atmospheric precipitation through the eastern Lunshan Reservoir. The thermal water is SO_4–Ca type and is formed by deep groundwater circulation along the NW and SN faults, which is heated by a geothermal gradient or hydrolysis of sulfide minerals such as pyrite and has little influence on the activity of shallow groundwater. Carbonate and anhydrite dissolutions occur in the circulation and they dominate the water–rock interaction processes in the geothermal reservoir. The hot water in the fractured rock has strong dissolution ability, and

fissures, small karst caves, and broken cores have developed in the water circulation area. In addition, on the basis of previous studies and the comparative analysis of topography, formation of lithologies, geological structures, and hydrogeological conditions of low-medium temperature hot springs around Nanjing, it can also be found that the origin of the four hot spring groups in karst landforms have many similarities. Exploring the origin of hot springs in karst areas around Nanjing, and figuring out their similarities and distribution characters are the basis of rational planning of the amount of geothermal water and cold groundwater water exploitation. The results are significant in further research, and they can also improve the accuracy and efficiency of exploration and development of the geothermal resources in karst landform around Nanjing. In the further research, the connections of four hot spring groups need to do be studied using isotopic method, and the influence of rainy and dry seasons on the groundwater need to be considered. The relationship between surface water, cold karst groundwater, and geothermal water is also under consideration.

Acknowledgments: Thanks for the support from Huadong Engineering Corporation Limited, China. Thanks for the support from Prof. Jinzhong Tan and the colleagues from The 1st Geological Brigade of Jiangsu Geology & Exploration Bureau, Nanjing, China.

Funding information: This research received no external funding.

Author contributions: J.M. and Z.Z. conceived and designed the study; J.M. collected and analyzed the data; J.M. wrote the paper with the assistance of Z.Z.

Conflict of interest: The authors declare that there are no conflicts of interest regarding the publication of this paper.

References

[1] Akhtar MN, Akhtar J, Tarannum N. Physiochemical characterization and dematerialization of coal class F flyash residues from thermal power plant. Civil Engineering J. 2019;5(5):1041–51.

[2] Dublyansky YV. Karstification by geothermal waters. Treatise Geomorphol. 2013;6:57–71.

[3] Ford D, Williams P. Karst hydrogeology and geomorphology. Chichester, England: John Wiley and Sons Ltd.; 2007. p. 1–562.

[4] Goldscheider N, Mádl-Szonyi J, Eross A, Schill E. Review: thermal water resources in carbonate rock aquifers. Hydrogeol J. 2010;18(6):1303–18.

[5] Caine JS, Evans JP, Forster CB. Fault zone architecture and permeability structure. Geology. 1996;24(11):1025–8.

[6] Pasvanoğlu S, Çelik M. Hydrogeochemical characteristics and conceptual model of Çamlıdere low temperature geothermal prospect, northern central Anatolia. Geothermics. 2019;79:82–104.

[7] Fazelabdolabadi B, Golestan MH. Towards Bayesian quantification of permeability in micro-scale porous structures–the database of micro Networks. HighTech Innovat J. 2020;1(4):148–60.

[8] Houria B, Mahdi K, Zohra TF. Hydrochemical characterisation of groundwater quality: Merdja plain (Tebessa Town, Algeria). Civil Eng J. 2020;6(2):318–25.

[9] Guo Q, Wang Y, Liu W. O, H, and Sr isotope evidences of mixing processes in two geothermal fluid reservoirs at Yangbajing, Tibet, China. Environ Earth Sci. 2010;59(7):1589–97.

[10] Reinsch T, Henninges J, Ásmundsson R. Thermal, mechanical and chemical influences on the performance of optical fibres for distributed temperature sensing in a hot geothermal well. Environ Earth Sci. 2013;70(8):3465–80.

[11] Kong Y, Pang Z, Shao H, Hu S, Kolditz O. Recent studies on hydrothermal systems in China: a review. Geotherm Energy. 2014;2(1):1–12.

[12] Lu L, Pang Z, Kong Y, Guo Q, Wang Y, Xu C, et al. Geochemical and isotopic evidence on the recharge and circulation of geothermal water in the Tangshan geothermal system near Nanjing China: implications for sustainable development. Hydrogeol J. 2018;26(5):1705–19.

[13] Yang P, Cheng Q, Xie S, Wang J, Chang L, Yu Q. Hydrogeochemistry and geothermometry of deep thermal water in the carbonate formation in the main urban area of Chongqing, China. J Hydrol [Internet]. 2017;549(June):50–61. doi: 10.1016/j.jhydrol.2017.03.054.

[14] Worthington SRH, Ford DC. High sulfate concentrations in limestone springs: an important factor in conduit initiation? Environ Geol. 1995;25:9–15.

[15] Yoshimura K, Nakao S, Noto M, Inokura Y, Urata K, Chen M, et al. Geochemical and stable isotope studies on natural water in the Taroko Gorge karst area, Taiwan-chemical weathering of carbonate rocks by deep source CO_2 and sulfuric acid. Chem Geol. 2001;177(3–4):415–30.

[16] Boschetti T, Toscani L, Barbieri M, Mucchino C, Marino T. Low enthalpy Na-chloride waters from the Lunigiana and Garfagnana grabens, Northern Apennines, Italy: Tracing fluid connections and basement interactions via chemical and isotopic compositions. J Volcanol Geotherm Res. 2017;348:12–25. doi: 10.1016/j.jvolgeores.2017.10.008.

[17] Battistel M, Hurwitz S, Evans WC, Barbieri M. The chemistry and isotopic composition of waters in the low-enthalpy geothermal system of Cimino-Vico Volcanic District, Italy. J Volcanol Geotherm Res. 2016;328:222–9. doi: 10.1016/j.jvolgeores.2016.11.005.

[18] Wang G, Lin W, Zhang W, Liu Z, Ma F, Liang J, et al. Geothermy of China. Beijing: Science Press; 2018.

[19] Luan G, Qiu H. The type of low-medium temperature geothermal system of convection type, the genesis analysis of Tangshan geothermal system in Nanjing. J Ocean Univ Qingdao. 1998;28(1):156–60. (in Chinese with English summary).

[20] Zhao J, Zhu S. Control factors and resources prospect of geothermal water in Tangshan hill of Nanjing. Jiangsu Geo. 1998;22(4):242–8. (in Chinese with English summary).
[21] Li A, Zhu C, Yang S. The research on formation condition of Tangshan warm spring in Nanjing. Miner Explor. 2010;1(6):546–9. (in Chinese with English summary).
[22] Zou P, Qiu Y, Wang C. Analyses of the genesis of Tangshan hot spring area in Nanjing. Geol J China Univ. 2015;21(1):155–62. (in Chinese with English summary).
[23] Li H, Hong J. Discussion on the overall planning path of small towns in the outer edge of scenic resources: a case study of the north area of Laoshan in Nanjing. Dev Small Cities Towns. 2014;10:78–81. (in Chinese with English summary).
[24] Li L, Wang L. Analysis of formation causes of natural mineral water No 1 springs between Anhui province and Laoshan Double Spring of Xianxiang county. Ground Water. 2016;38(5):16–8. (in Chinese with English summary).
[25] Ding M, Zhu C. Analysis of forming geothermal favorable conditions in Liuhe area of Nanjing city. Ground Water. 2016;28(1):10–2. (in Chinese with English summary).
[26] Ge X. Nappe structures in the Ningzhen Mountains. J Changchun College Geol. 1987;17(2):143–54. (in Chinese with English summary).
[27] Zhou C, Yuan L, Liu Z, Zhang H. Evolution of landform and karst development in Tangshan. Nanjing. Sci Geogr Sin. 2006;26(1):47–51. (in Chinese with English summary).
[28] Pan S, Ding Z. Properties of geothermal geology in the areas of south Jiangsu. Jiangsu Geo. 2001;25(4):228–33. (in Chinese with English summary).
[29] Huang T, Pang Z, Liu J, Ma J, Gates J. Groundwater recharge mechanism in an integrated tableland of the Loess Plateau, northern China: insights from environmental tracers. Hydrogeol J. 2017;25(7):2049–65.
[30] Huang T, Pang Z, Li J, Xiang Y, Zhao Z. Mapping groundwater renewability using age data in the Baiyang alluvial fan, NW China. Hydrogeol J. 2017;25(3):743–55.
[31] Ma R, Wang Y, Sun Z, Zheng C, Ma T, Prommer H. Geochemical evolution of groundwater in carbonate aquifers in Taiyuan, northern China. Appl Geochemistry. 2011;26(5):884–97.
[32] Wang J. Low-medium temperature geothermal system of convective type. Earth Sci Front (China Univ Geosci Beijing). 1996;3(3–4):96–103. (in Chinese with English summary).
[33] Xiong L, Zhang J. Mathematical simulation of refract and redistribution of heat flow. Sci Geol Sin. 1984;4:445–54. (in Chinese with English summary).